JOURNAL OF CATALYSIS 107, 510–521 (1987)

Carbon Monoxide Methanation over $FeTi_{1+x}$ Intermetallics

R. SASIKALA, N. M. GUPTA, S. K. KULSHRESHTHA, AND R. M. IYER

Chemistry Division, Bhabha Atomic Research Centre, Bombay 400 085, India

Received January 19, 1987; revised May 6, 1987

$FeTi_{1+x}$ intermetallics ($0 \leq x \leq 0.15$), well-known hydrogen absorption materials, have been found to be active catalysts for CO methanation. The initial activity for H_2 absorption, CO disproportionation, and CO hydrogenation increased significantly with increasing Ti content. However, the catalysts rapidly lost their activity because of carbon layer deposition at the surface. Mössbauer and X-ray diffraction studies indicate that no surface or bulk carbides are formed during CO/H_2 reaction. Auger electron spectroscopy data have revealed that for all the titanium compositions, the surface is rich in iron, and conversion electron Mössbauer results showed that the surface becomes enriched with iron metal clusters during catalytic reaction. Thus, the catalytic activity is attributed to α-iron centers at the surface which are responsible for the formation of different carbonaceous precursor species. Excess Ti concentration results in the formation of secondary iron titanium suboxide phases which help in the generation of additional active sites during the activation process. The activity of surface carbon species and the reaction routes involved in CO methanation are discussed in detail.

INTRODUCTION

Many intermetallic compounds, such as $LaNi_5$, Mg_2Ni, and FeTi, reversibly absorb large amounts of hydrogen (*1–3*). The intermetallics owe their absorption property to the surface dissociation of hydrogen molecules, the adsorbed atoms diffusing subsequently into the bulk. In conformity with their hydrogen dissociation/absorption capacity, these materials would therefore be expected to catalyze hydrogenation reactions. It would be of interest to know whether the activity of these hydrogen storage materials merely depends on their hydrogen dissociation property or is also influenced by absorbed hydrogen. Indeed, intermetallic compounds such as RM_2, RM_3, and RM_5 (where R signifies a rare earth metal and M a transition metal such as Ni and Fe) are known to exhibit appreciable activity for catalytic reactions, such as the hydrogenation of nitrogen, carbon monoxide and hydrocarbons (*2–7*). During the CO hydrogenation process, the rare earth intermetallics continuously dissociate to form rare earth oxide and transition metal sites, the latter being the active centers for catalytic reaction. Thus unlike supported catalysts these systems are self-generative in nature (*2–8*). The intermetallic compound FeTi is known to have better hydrogen storage properties compared with most of the rare earth intermetallics (*1*). Different views have been expressed to explain the mechanism of hydrogen storage and activation of FeTi. Some authors (*9*) believe that the existence of superparamagnetic clusters of Fe metal below the Ti-rich outer surface layers is responsible for the dissociation of hydrogen, while others emphasize the role of suboxides of iron and titanium existing on the surface of FeTi (*10, 11*), particularly for titanium-rich compositions (*12, 13*).

There have been conflicting views on the chemical identity of the surface centers which are responsible for the catalytic activity of iron for the Fischer–Tropsch (FT) process. Depending on the composition, pretreatment, temperature, and CO/H_2 ratio, the surfaces of different iron catalysts are known to contain a mixture in varying proportions of iron oxide, iron carbide, and

0021-9517/87 $3.00

a small amount of α-iron (*14*), though there has been no unanimity of view as to which of these centers are responsible for catalytic activity. Tau and Bennett (*15*) have shown that the support plays an important role in determining the nature of surface species formed during the CO/H_2 reaction. Bonzel and Krebs (*16*) and Dwyer and Somorjai (*17*) have demonstrated that in the H_2/CO reaction over polycrystalline iron foils, α-iron is the active center which becomes deactivated on deposition of surface carbon. However, in the case of iron powders, the reaction was considered to be followed by the formation of carbidic carbon (*18*). Raupp and Delgass (*19*) and Amelse *et al.* (*20*) have demonstrated a correlation between the extent of carbide formation and the activity of the catalyst for FT reaction. Reymond *et al.* (*21*) suggest that iron oxides are the necessary components of the working iron catalysts while Dictor and Bell (*14*) have demonstrated that potassium-promoted and unpromoted iron oxide are good FT catalysts.

Niemantsverdriet *et al.* (*22, 23*) have put forward a competition model which considers the surface iron atoms as active sites. It is proposed that after adsorption and dissociation of CO, the surface carbon atoms may (i) diffuse into the bulk to form a bulk carbide, (ii) react with chemisorbed hydrogen atoms to form hydrocarbon precursor species (e.g., CH_x), or (iii) convert to a nonreactive graphitic form. Matsumoto and Bennett (*24*) have similarly demonstrated that in FT synthesis over commercial fused iron catalysts the surface consists of metallic iron, though the bulk converts to Hägg carbide (Fe_2C). Using a transient method, these authors have shown that methanation and the FT reactions over fused iron take place via surface carbon intermediates which become deactivated in the absence of H_2.

The questions which attracted our attention were (i) whether the FeTi system would be an effective hydrogenation catalyst like rare earth intermetallics, and (ii) just as excess Ti in FeTi facilitates the H_2 activation process (*12, 13*), would it also result in the enhanced hydrogenation activity of these materials? The identification of the surface centers responsible for chemisorption and reaction of hydrogen and CO on FeTi and reaction routes leading to the formation of CH_4 have also been the subject of this study. The present paper deals with the evaluation of CO hydrogenation activity of $FeTi_{1+x}$ alloys ($0 \leq x \leq 0.15$). These compositions were chosen because their hydrogen storage properties are well known (*1, 12, 13*). The samples were characterized before and after catalysis experiments using the techniques of Mössbauer spectroscopy, X-ray diffraction, and Auger electron spectroscopy. The preliminary results of this study have been reported earlier (*25*). In very recent studies Hirata (*26, 27*) has observed the formation of different hydrocarbons on the $FeTi_{1.14}O_{0.03}$ surface when impure hydrogen containing a few hundred parts per million of CO, CO_2, and O_2 was used for hydriding the sample.

EXPERIMENTAL

Sample preparation. Samples of $FeTi_{1+x}$ with x = 0.0, 0.05, 0.10, and 0.15 were prepared from electrolytic grade Ti and freshly reduced iron powder of high purity by repeated arc melting. The ingots so prepared were annealed at about 1175 K for 7 days in evacuated quartz tubes for homogenization. Chemical analysis and electron probe microanalysis were used to confirm the compositions of different alloy samples.

Chemisorption and surface area. The evaluation of the active surface area of fresh and H_2-activated samples was attempted by the CO pulse adsorption method at room temperature. The hydrogen absorption capacity (at atmospheric pressure and 300 K) of samples was also determined using thermal desorption spectroscopy. For this purpose, the samples were heated in H_2 for 2–3 h at 625 K and

cooled in H_2 to 300 K. At this stage, the sample was allowed to equilibrate in flowing He. Absorbed hydrogen was measured by desorption upon reheating to 950 K at a uniform rate of 30 K min^{-1}.

Catalytic activity. For evaluation of the catalytic activity powdered samples having a particle size between 150 and 300 mesh were used in a microcatalytic reactor, described earlier in detail (*28*). For each experiment 3 g of the sample was placed in a 0.3-cm-i.d. stainless-steel tube reactor, connected in series to gas sampling valves, injection ports, a Porapak-Q column, and a thermal conductivity detector. The configuration of gas sampling valves could be modified either to use them for injecting reactant gas pulses over the catalyst sample or to analyze the effluent product gases.

The methanation reaction was conducted in two different modes. In one mode, 40-μl CO pulses were periodically injected into a hydrogen stream (32 ml min^{-1}) flowing over the catalyst bed. In the second mode, the CO + H_2 gas mixture (1 : 3.8) was continuously reacted over the catalyst bed at a flow rate of 9–10 ml min^{-1}. In both these modes the reactor pressure was nearly 1 atm. The effect of regeneration treatment was investigated by heating the catalyst *in situ* at 625 K for about 2 h each, under O_2 and H_2 flow (45 ml min^{-1}) in succession. Under present experimental conditions and with the CO/H_2 ratio used, the main reaction product was methane. Higher hydrocarbons were not observed in our experimental setup, indicating that if formed, they were only in trace quantities.

Reaction intermediates. To evaluate the nature of surface species formed in the interaction of CO with catalyst surface, the following experiments were performed. After *in situ* regeneration of the catalysts the carrier gas flow was switched to He (35 ml min^{-1}) while the sample was maintained at 625 K. After ascertaining that all the adsorbed H_2 had been released, pulses of CO were injected over the catalyst surface and the effluent was analyzed. After injection of a CO pulse and release of the products formed, successive H_2 pulse injections were made and the reaction products were analyzed again. Variation of the time interval between CO and H_2 pulse injection gave information about the time-dependent variation in reactivity of the surface species formed over the catalyst surface on exposure to CO.

Gases. High-purity H_2 gas from Indian Oxygen was used after further purification with a Matheson Model 8362 hydrogen purifier. Helium from Airco was used after passage through a deoxo catalyst (500 K) and a molecular sieve trap. High-purity carbon monoxide, also from Airco, was used without further treatment.

Catalyst characterization. Transmission γ-ray and conversion electron ^{57}Fe Mössbauer spectra were recorded to determine changes in chemical states and for phase identification in fresh and used catalyst samples using a constant-acceleration Mössbauer spectrometer with a ^{57}Co source in a Rh matrix. A conventional X-ray diffractometer with a Cu $K\alpha$ source was used to record diffraction patterns of original fresh and deactivated samples. Auger electron spectroscopy (AES) studies were carried out on air fractured alloy pieces of about 4 × 4 mm using a PHI 551 electron spectrometer employing a 3-keV electron beam. Depth profiles of different elements were recorded after *in situ* 1-keV argon ion sputtering.

RESULTS

Adsorption and Catalysis

Surface area and hydrogen adsorption. CO adsorption on the catalyst was found to be negligible at room temperature. The temperature programmed desorption of hydrogen gave a broad spectrum with two maxima at about 525 K and 800 K (*29*). The total amount of hydrogen desorbed was found to increase with increasing titanium content. The amount of hydrogen desorbed from samples with x = 0.0, 0.05, 0.10 and

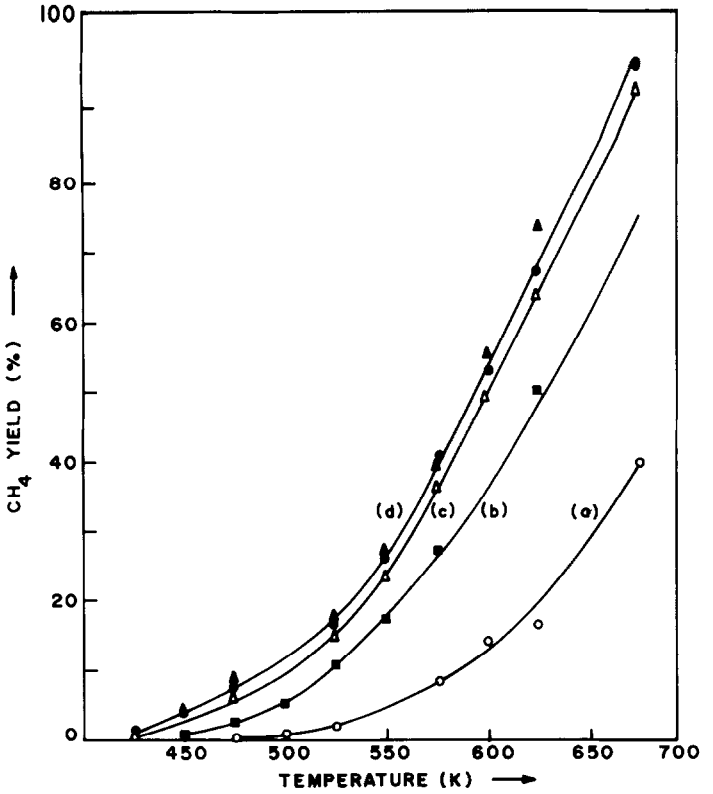

FIG. 1. Effect of successive oxygen and hydrogen regeneration cycles (625 K, 2 h) on CO methanation activity of $FeTi_{1.05}$ catalyst: (a) ○, no initial regeneration, (b) ■, first regeneration, (c) △, second regeneration, (d) ●, third regeneration, ▲, fourth regeneration.

0.15, was found to be approximately 2.0, 5.6, 7.9 and 13.5 ml g^{-1} respectively. The total surface area of all these samples as evaluated by N_2 adsorption using the BET method, was around 0.5 $m^2 g^{-1}$. It is therefore apparent that part of the adsorbed H_2 has diffused in the matrix bulk even under conditions of atmospheric pressure and 300 K.

Catalytic activity. Curve a in Fig. 1 shows the percentage methane yield obtained when 40-μl CO pulses were injected into H_2 carrier gas over freshly ground $FeTi_{1.05}$ catalyst at different temperatures. At this stage when the sample was subjected to *in situ* O_2 and H_2 regeneration treatments (625 K, 2 h), the catalyst activity was found to improve. Maximum catalyst activity was achieved after three or four such regeneration treatments (Fig. 1). Similar regeneration effects were observed with alloys of other compositions. Increasing Ti content had a promotional effect on the catalytic activity and the data for different sample compositions are given in Fig. 2. The methane yield in this figure refers to saturation yields observed after the fourth regeneration cycle, as mentioned above.

Arrhenius plots of the data in Figs. 1 and 2 show that the CO methanation is a two-step process, the activation energy values decreasing with increasing titanium content and on progressive regeneration treatments. Thus, for an increase in Ti/Fe ratio from 1 to 1.15, the apparent activation energy for one of the steps was found to decrease from about 25.2 to 21 kJ mol^{-1} while the value for the other step decreased progressively from 53.3 to 45.0 kJ mol^{-1}.

When CO/H_2 mixture (1 : 3.8) was re-

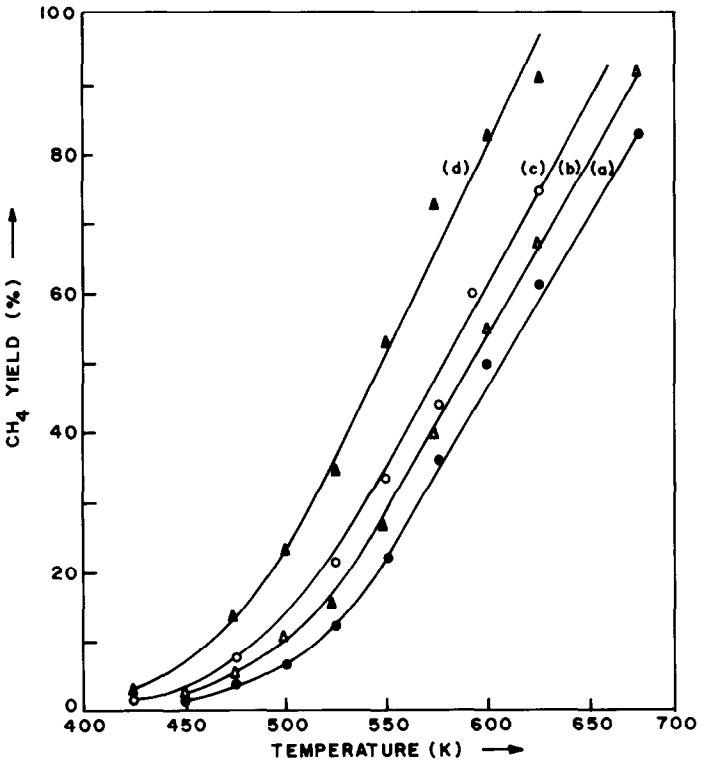

FIG. 2. CO methanation activity of $FeTi_{1+x}$ intermetallics at different temperatures in the presence of excess hydrogen: (a) $x = 0$, (b) $x = 0.05$, (c) $x = 0.10$, (d) $x = 0.15$.

acted over the catalyst surface, CH_4 and CO_2 were the observed products (no attempts were made to detect moisture, if formed). The yields of both CH_4 and CO_2 were found to decrease rapidly with time. The typical behavior of catalyst deactivation at two different temperatures is shown in Fig. 3 for a $FeTi_{1.15}$ sample. It is interesting to note that after a very rapid fall in activity during first 20 min, the catalyst maintains its low level activity for several hours. Also, at the stage where the steep fall in CH_4 yield is observed, the CO_2 yield was also found to be considerably reduced. It may also be noted that the CO_2 yield is higher at 575 K than at 625 K.

Disproportionation of CO and hydrogenation of surface species. When 40-μl CO pulses were injected over catalyst samples in the presence of He carrier gas, CO_2 was found to be formed. The CO_2 yields and the

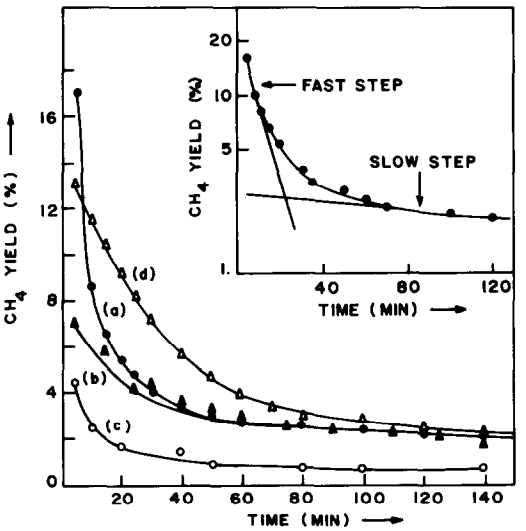

FIG. 3. CH_4 (a, b) and CO_2 (c, d) yields obtained when CO + H_2 (1:3.8) gas mixture is reacted over $FeTi_{1.15}$ at 625 K (a, c) and 575 K (b, d). The inset shows a semilog plot of curve a.

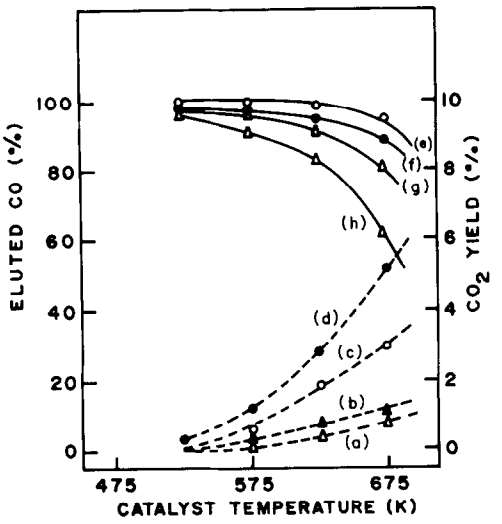

FIG. 4. Yields of CO_2 (a–d) and unreacted CO (e–h) obtained when 40-μl CO pulses were injected over FeTi at different temperatures: (a, e) no regeneration, (b, f) after first regeneration, (c, g) after second regeneration, (d, h) after third regeneration.

amount of eluted unreacted CO in the effluent are given in Figs. 4 and 5 for two representative compositions of FeTi and $FeTi_{1.15}$ respectively after different regeneration treatments.

From these figures it is clear that the efficiency of the catalyst for CO dissociation increases on regeneration treatment and with increasing Ti content. It is also important to note that the amount of CO_2 formed at different temperatures is far less than the amount of CO consumed, implying that significant amounts of carbon and oxygen are deposited or reacted over the catalyst surface in the process.

Subsequent to a CO pulse injection in He carrier gas, as mentioned above, a hydrogen pulse (referred to as first hydrogen) was injected over the catalyst bed and formation of CH_4 was observed. When further H_2 pulse injections were made at 2-min intervals, decreasing amounts of CH_4 were formed. An increase in catalyst temperature gave rise to higher CH_4 yields. However, at any particular temperature when the time interval between CO and the first H_2 injection was increased, the methane yields were found to decrease progressively. Typical data for the variation of methane yields for successive H_2 injections are given in Table 1 for a sample of $FeTi_{1.15}$. A similar variation in the CH_4 yield on changing the CO–H_2 pulse interval had been observed in earlier investigations using Ru catalysts (*30*).

CO/H_2 reaction over preoxidized surface. To evaluate the role of surface oxides in methanation, the catalyst samples were heat treated in O_2 (625 K, 1 h) and then in He (625 K, 2 h). The pulses of CO + H_2 (1 : 5) (or CO alone) were injected over the catalyst bed in the presence of He. Formation of CH_4 was not observed at all reaction temperatures up to 675 K; the effluent contained CO_2 in addition to unreacted CO and H_2. Typical results obtained for FeTi are given in Table 2. These results indicate that under present experimental conditions the CO would primarily reduce surface metal oxide to the metallic form rather than itself reducing to CH_4.

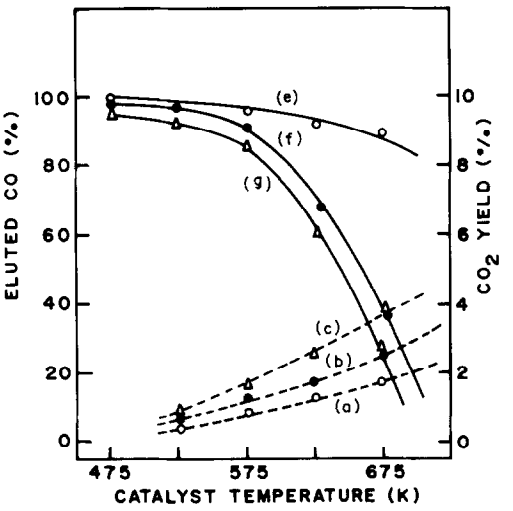

FIG. 5. Yields of CO_2 (a–c) and unreacted CO (e–g) obtained when 40-μl CO pulses were injected over $FeTi_{1.15}$ at different temperatures: (a, e) no regeneration, (b, f) after first regeneration, (c, g) after second regeneration.

TABLE 1

Methane Yields Obtained on Injection of 40 μl CO on $FeTi_{1.15}$ at 675 K followed by Successive Injections of 160 μl of H_2

Time interval between CO and first H_2 pulse injection (min)	Sequential number of hydrogen pulse						Total CH_4 yield (μl)
	1	2	3	4	5	6	
0	6.2[a]	2.6	1.7	1.0	0.6	0.4	12.5
1	3.5	1.8	1.2	0.9	0.6	0.6	8.6
5	2.6	1.9	1.0	0.7	0.5	0.4	7.1
10	2.2	1.8	1.0	0.7	0.5	0.3	6.5
30	1.1	1.1	0.8	0.6	0.4	0.3	4.3

[a] Values are expressed in μl $\pm$ 0.05.

Sample Characterization

Mössbauer results. Mössbauer spectra of original $FeTi_{1+x}$ samples in the transmission mode are shown in Fig. 6 and suggest that there is no change in the lineshape due to excess Ti. The single line with isomeric shift $\delta = -0.13$ mm s^{-1} (with respect to Fe metal at room temperature) is typical of the FeTi phase (*31*). The Mössbauer spectra of these samples recorded after deactivation in continuous CO/H_2 reaction (625 K, 6 h) were identical to those shown in Fig. 6, showing no formation of bulk carbide or oxide during CO hydrogenation.

Figure 7 shows the conversion electron Mössbauer spectra of two of the representative samples before and after complete deactivation. In the spectra for the samples used, a very weak magnetic pattern due to Fe metal clusters is discernible in addition to the usual single line for FeTi. Within the detection limits of these experiments, iron oxide or carbide formation was not observed. Niemantsverdriet *et al.* (*32*), however, have shown that Mössbauer spectra of unsupported iron catalysts after FT synthesis show contributions of iron oxide only when the spectra are recorded at 4.2 K. A very small concentration of iron oxide if formed at the surface may therefore go undetected in our Mössbauer study.

XRD results. Figure 8 shows a selective region of the X-ray diffraction (XRD) pat-

TABLE 2

CO/H_2 Reaction at 625 K on the Preoxidized Surface of FeTi[a]

Pulse No.	Pulse composition	CO eluted (μl)	CO_2 yield (μl)	CH_4 yield (μl)
1	$CO + H_2$	19.4	20.1	Nil
2	$CO + H_2$	30.0	9.5	Nil
3	CO	34.4	5.3	Nil
4	CO	34.2	4.5	Nil

[a] CO amount in each pulse = 40 μl.

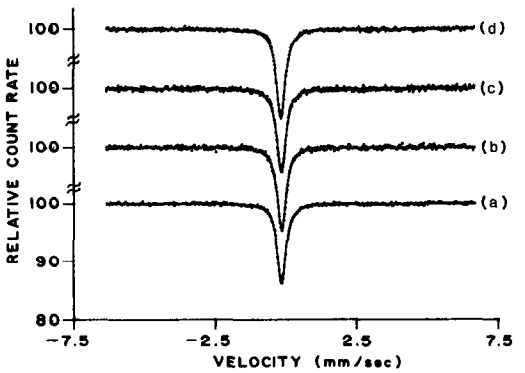

FIG. 6. Transmission Mössbauer spectra of as-prepared $FeTi_{1+x}$ intermetallics: (a) $x = 0.0$, (b) $x = 0.05$, (c) $x = 0.10$, (d) $x = 0.15$.

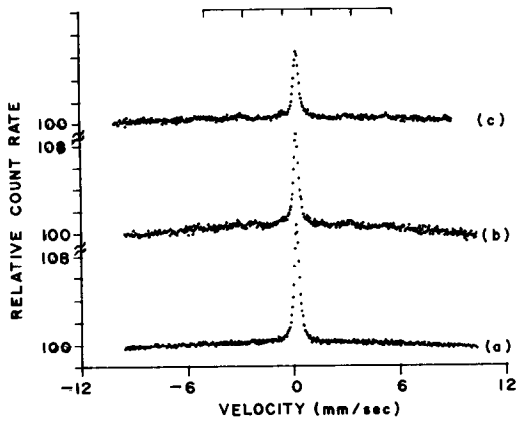

FIG. 7. Conversion electron Mössbauer spectra of (a) original FeTi sample, (b) FeTi after catalysis experiments, and (c) $FeTi_{1.05}$ after catalysis experiments. Peak positions of Fe metal are marked at the top.

terns of freshly powdered samples of $FeTi_{1+x}$ recorded just before they are loaded in the catalytic reactor. From this figure it is clear that our sample of FeTi is indeed a single phase with $a = 2.966$ Å, but the samples with excess Ti show small additional lines at $2\theta = 39.2$, 41.6, and 45.2°. The intensity of these reflections was found to increase systematically with increase in Ti content. These peaks cannot be indexed in terms of α-Ti or cubic β-Ti (with extrapolated values of $a = 3.283$ Å at room temperature). These reflections are characteristic of suboxides of $FeTiO_x$ (*11, 33, 34*) which is distributed in the bulk matrix of FeTi.

The XRD patterns of alloy samples remained unchanged on complete deactivation in CO/H_2 flow experiments, though the color of these samples had changed to blackish gray. This implies that unlike rare earth intermetallics, FeTi does not undergo chemical transformation, i.e., there is no substantial formation of bulk carbides or oxides of Fe and Ti, which is in conformity with the Mössbauer results.

Auger electron spectroscopy. An overall Auger spectrum of a fresh FeTi sample is given in Fig. 9a which shows the presence of C, O, and Fe at the surface while only a very small signal due to Ti is seen. The valley-shaped C signal at 272 eV in this spectrum is a characteristic of a multilayer surface carbon deposit (*17, 35*). Ar^+ sputtering gave rise to an increase in both Ti and Fe signals and significant reduction in O and C peaks. Spectra b and c in Fig. 9 show the data recorded after 15 and 60 min of Ar^+ sputtering. Elemental depth profiles were also recorded in terms of atom concentration while samples were under argon ion sputtering. The ratios of iron to titanium atom concentration after different surface sputterings are given in Table 3.

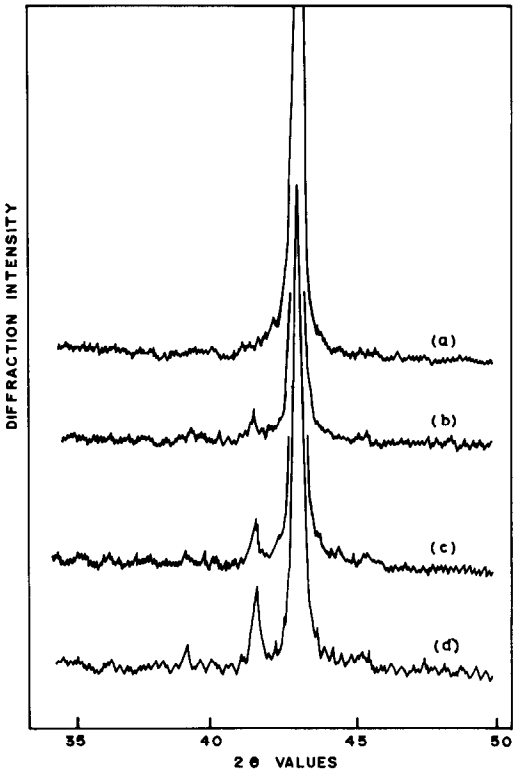

FIG. 8. X-ray diffraction pattern around (110) reflection region for different $FeTi_{1+x}$ intermetallics: (a) $x = 0.0$, (b) $x = 0.05$, (c) $x = 0.10$, (d) $x = 0.15$.

The $FeTi_{1+x}$ samples cleaned by argon ion sputtering (Fig. 9c) when exposed to CO gas at temperatures higher than 500 K gave a large carbon signal in the Auger spectrum. Figure 9d shows an Auger spectrum from a FeTi sample exposed to CO/He

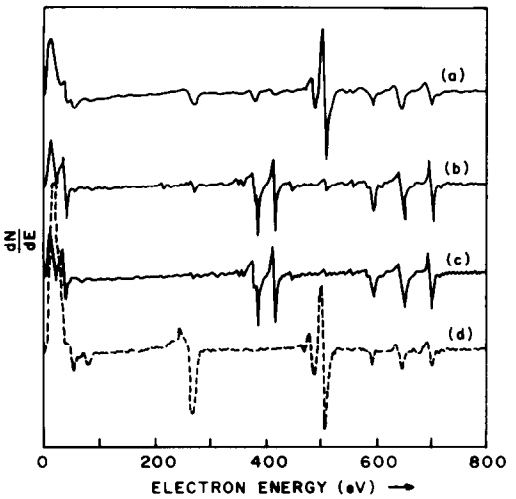

FIG. 9. Auger electron spectra of FeTi catalyst: (a) no treatment; (b and c) after 15 and 60 min argon ion (1 keV) sputtering; (d) sputter-cleaned and exposed to CO/He at 575 K. C (272 eV), Ti (383, 387, 418 eV), O (510 eV), Fe (598, 651, 703 eV).

flow (1 : 4, 30 ml min^{-1}) at 575 K for 60 min. The intensity of the carbon signal was again drastically reduced on Ar^+ sputtering, indicating that the carbon deposited on CO exposure is located only on the surface.

DISCUSSION

The following are the important points of interest in this study.

1. The methanation activity of Fe–Ti alloys increases with increase of the Ti/Fe ratio from 1 to 1.15. This behavior finds a parallelism in excess Ti-induced ease of activation of these alloys (*12, 13*) for hydrogen storage which is reflected in higher hydrogen absorption in Ti-rich samples as mentioned under Surface Area and Hydrogen Adsorption.

2. Unlike rare earth intermetallics, no component of $FeTi_{1+x}$ undergoes a major chemical transformation during the CO/H_2 reaction.

3. Iron catalysts, in both supported and unsupported forms, are known to transform easily into carbide form during $CO–H_2$ reaction, the nature of the carbide depending on various factors such as catalyst support, CO/H_2 ratio, and temperature. In our Mössbauer study, although the formation of iron clusters is revealed, no iron carbide or oxide phases were detected at the catalyst surface and these phases are therefore unlikely to be responsible for CO hydrogenation.

4. Auger spectra show that irrespective of Ti content, all the alloys have an iron-rich surface, at least a part of which may be in the suboxide form.

5. A parallelism in higher hydrogen adsorption capacity (see Surface Area and Hydrogen Adsorption) and higher CO dissociation efficiency (Fig. 5) of Ti-rich samples indicates that the centers responsible for H_2 dissociation are probably the same as those where CO is adsorbed and dissociated.

6. Exposure to CO results in the formation of a surface carbonaceous layer (Fig. 9) which only in its nascent form is active for methanation. The data of Table 1 show that with time the surface carbon converts to an inactive form (*23, 29*).

7. Arrhenius plots of the data in Fig. 2 and the semilog plot of the data in Fig. 3 indicate that both methanation and catalyst deactivation are two-step processes. The activation energy for methanation decreased with increasing Ti content of $FeTi_{1+x}$ and the progressive O_2/H_2 regeneration treatment.

These results can be rationalized if we assume that iron metal centers are respon-

TABLE 3

Ratios of Iron to Titanium Atom Concentration (Fe/Ti) in Different Alloys as a Function of Argon Ion Sputtering[a]

Sputtering time (min)	FeTi	$FeTi_{1.10}$	$FeTi_{1.15}$
0	2.70	2.50	3.55
10	1.30	1.25	0.96
40	1.15	1.10	0.94

[a] Sputtering rate ≈25 Å per minute.

sible for H_2 and CO dissociation and their surface reaction (*23, 24*). The increase in catalytic activity with excess titanium compositions may be ascribed to the existence of a secondary suboxide phase in the matrix. From hydrogen absorption studies it has been reported that the existence of the secondary phase facilitates the activation of samples for hydrogen loading (*33*) as the suboxides first become hydrogenated and create strains in the matrix. The strains produced in the lattice create microcracks, thus enhancing the surface sites for dissociation of H_2 and possibly for CO also. However, as the oxygen content of these suboxides is too small to affect the values of isomeric shift, Mössbauer studies do not reveal their existence as a separate phase. Some of the suggested suboxides are $Fe_5Ti_7O_2$ (*34*), Fe_3Ti_3O, Fe_2Ti_4O (*36*), and $Fe_7Ti_{10}O_3$ (*26*). It is of interest to observe that the fast-step activation energy value of about 22 kJ mol^{-1} as evaluated from the data in Fig. 2 is very close to the values reported by Vannice for CO methanation over different Fe/TiO_2 samples (*37*), in contrast to the higher activation energy values (84–100 kJ mol^{-1}) reported in the literature for iron supported over other materials (*15, 37–39*). It can therefore be concluded that the catalyst surface in our study consists of iron clusters (active sites) held on the titanium and iron oxide centers via strong metal–support interaction. The increasing titanium content would give rise to better dispersion of iron clusters and hence would result in enhanced hydrogen decomposition and its subsequent absorption. The repeated O_2/H_2 regeneration cycles would also generate a larger number of surface Fe/TiO_x centers, resulting in enhanced catalytic activity as has been observed in our study (Fig. 1). Auger electron spectroscopy studies have indeed revealed the surface formation of titanium oxide and to some extent of iron oxide upon exposure of intermetallics to CO or oxygen (*29*).

The multiple-step catalytic methanation and subsequent deactivation process seen in Figs. 2 and 3 may have its origin in any of the following: (i) two types of active sites, (ii) two types of surface carbon species, or (iii) slower transport of CO and H_2 to metal sites due to a carbon layer barrier. Tau and Bennett (*40*) have suggested the formation of at least two types of reaction intermediates, referred to as CH_x and CH_y ($0 \leq x, y \leq 3$), one of them being more reactive than the other. H_2 thermal desorption spectra of all the samples gave two desorption peaks at 575 and 775 K, indicating the existence of at least two different adsorption/absorption sites.

It is now generally accepted [for a review, see Ref. (*41*)] that the reactants in the CO/H_2 reaction are dissociatively chemisorbed on the catalyst as atomic carbon, oxygen, and hydrogen. Surface oxygen can be removed by one of the following reactions.

$$O_{ad} + CO_{ad} \rightarrow CO_2 \quad (1)$$

$$O_{ad} + 2H_{ad} \rightarrow H_2O \quad (2)$$

$$O_{ad} + Fe_{(s)} \rightarrow Fe_{(s)}\text{–}O \quad (3)$$

$$O_{ad} + Ti_{(s)} \rightarrow Ti_{(s)}\text{–}O \quad (4)$$

$$Fe_{(s)}\text{–}O + CO_{ad} \rightarrow CO_2 + Fe_{(s)} \quad (5)$$

$$Fe_{(s)}\text{–}O + 2H_{ad} \rightarrow H_2O + Fe_{(s)} \quad (6)$$

The present data show that the predominance of any of these steps would depend on experimental conditions. In the case when no H_2 is available, oxygen would react with surface iron or titanium centers (Figs. 4, 5). Auger results have confirmed that on interaction with CO and also with CO/H_2, the alloy surface contains oxided iron and titanium (*29*). However, in the presence of CO/H_2, reactions (5) and (6) would play an important role in keeping the iron centers in metallic form and permitting step (1) to produce CO_2. The heat of formation (ΔH_f^0) values of FeO and CO_2 are -267.5 and -396.8 kJ mol^{-1}, respectively, indicating that Fe and CO would compete to take up adsorbed oxygen. The results with the preoxidized surface (Table 2)

clearly show that surface iron oxide can be reduced further on exposure to CO.

The data in Fig. 3 show that in continuous CO/H_2 experiments the yield of CO_2 is greater at lower temperatures, thus indicating that at higher temperatures the CO_2 is again methanated; this is also reflected in the yield of methane at higher temperatures. This was also confirmed from separate experiments conducted with a CO_2 and H_2 gas mixture. Dwyer and Somorjai (*17*) have indeed shown that even an iron foil has considerable activity for CO_2 methanation.

The data in Fig. 3 also indicate that FeTi intermetallics show maximum activity at the beginning of $CO + H_2$ reaction and do not require an activation period. On the contrary, supported metallic iron catalysts are found to show an initial low activity for FT synthesis, which according to the competition model of Niemantsverdriet *et al.* (*22, 23*) is attributable to initial diffusion and consumption of surface carbon atoms to form bulk carbides. The absence of an activation period in our study, combined with the finding that bulk carburization does not occur in $FeTi_{1+x}$, tends to support the competition model.

The surface carbon species may react with hydrogen to give methane either by stepwise insertion of each hydrogen or by simultaneous reaction with more than one atom.

(a)
$$C_{ad} + H_{ad} \rightarrow (CH)_{ad} \quad (7)$$
$$(CH)_{ad} + H_{ad} \rightarrow (CH_2)_{ad} \quad (8)$$
$$(CH_2)_{ad} + H_{ad} \rightarrow (CH_3)_{ad} \quad (9)$$
$$(CH_3)_{ad} + H_{ad} \rightarrow CH_4 \quad (10)$$

(b)
$$C_{ad} + xH_{ad} \rightarrow CH_x \quad (11)$$
$$(1 < x \leq 4)$$

The data in Fig. 3 show that the residual activity of the catalyst after abrupt poisoning (slow step) almost overlaps in experiments carried out at different temperatures. It has also been observed that although the samples containing excess Ti initially gave higher CH_4 yields in continuous CO/H_2 reaction, the yields corresponding to the slow step were almost the same for all $FeTi_{1+x}$ samples. The ease of hydrogen activation observed in titanium-rich samples would make more H_{ad} species available at a particular temperature and would thus facilitate route b. It may thus be surmised that route b plays a more important role in the initial stages of CO/H_2 reaction while stepwise hydrogen insertion may become predominant with progressive catalyst deactivation and may be identified with the slow step of Fig. 3. These views find support in the CO methanation study of Wang *et al.* (*42*) using Pd/TiO_2 catalyst, where it is suggested that the higher surface concentration of hydrogen compensates for reduced CO coverage, thus promoting CH_4 formation.

ACKNOWLEDGMENTS

We thank Mr. V. S. Kamble for his help in gas chromatography measurements and recording thermal desorption spectra. Thanks are also extended to Dr. S. K. Sharma for recording Augar electron spectra. The valuable comments of the referees are gratefully acknowledged.

REFERENCES

1. Schlapbach, L., and Riesterer, T., *Appl. Phys. A* **32,** 169 (1983).
2. Wallace, W. E., Elattar, A., Imamura, H., Craig, R. S., and Moldovan, A. G., *in* "Science and Technology of Rare Earth Materials," p. 329. Academic Press, New York, 1980.
3. Elattar, A., Wallace, W. E., and Craig, R. S., *Adv. Chem. Ser.* **178,** 7 (1979).
4. Barrault, J., Duprez, D., Percheron-Guegan A., and Achard, J. C., *J. Less-Common Met.* **89,** 537 (1983).
5. Barrault, J., Guilleminot, A., Percheron-Guegan, A., Paul-Boncour, V., and Achard, J. C., *Appl. Catal.* **22,** 263 (1986).
6. Barrault, J., Guilleminot, A., Achard, J. C., Paul-Boncour, V., Percheron-Guegan, A., Hilaire, L., and Coulon, M., *Appl. Catal.* **22,** 273 (1986).
7. Coon, V. T., Takeshita, T., Wallace, W. E., and Craig, R. S., *J. Phys. Chem.* **80,** 17 (1976).
8. Chin, R. L., Elattar, E., Wallace, W. E., and Hercules, D. M., *J. Phys. Chem.* **84,** 2895 (1980).

9. Schlapbach, L., Seiler, A., Stucki, F., and Siegmann, H. C., *J. Less-Common Met.* **73,** 145 (1980).
10. Schober, T., and Westlake, D. G., *Scr. Met.* **15,** 913 (1981).
11. Venkert, A., Dariel, M. P., and Talianker, M., *J. Less-Common Met.* **103,** 361 (1980).
12. Mizuno, T., and Morozumi, T., *J. Less-Common Met.* **84,** 237 (1982).
13. Raj, P., Satyamoorthy, A., Suryanarayana, P., Singh, A. J., and Iyer, R. M., *J. Less-Common Met.* **130,** 139 (1987).
14. Dictor, R. A., and Bell, A. T., *J. Catal.* **97,** 121 (1986).
15. Tau, L. M., and Bennett, C. O., *J. Catal.* **89,** 285 (1984).
16. Bonzel, H. P., and Krebs, H. J., *Surf. Sci.* **117,** 639 (1982).
17. Dwyer, D. J., and Somorjai, G. A., *J. Catal.* **52,** 291 (1978).
18. Dwyer, D. J., and Hardenbergh, J. H., *J. Catal.* **87,** 66 (1984).
19. Raupp, G. B., and Delgass, W. N., *J. Catal.* **58,** 348, 361 (1979).
20. Amelse, J. A., Butt, J. B., and Schwartz, L. H., *J. Phys. Chem.* **82,** 558 (1978).
21. Reymond, J. P., Menauleau, P., and Teichner, S. J., *J. Catal.* **75,** 39 (1982).
22. Niemantsverdriet, J. W., van der Kraan, A. M., van Dijk, W. L., and van der Braan, H. S., *J. Phys. Chem.* **84,** 3363 (1980).
23. Niemantsverdriet, J. W., and van der Kraan, A. M., *J. Catal.* **72,** 385 (1981).
24. Matsumoto, H., and Bennett, C. O., *J. Catal.* **53,** 331 (1978).
25. Kulshreshtha, S. K., Gupta, N. M., Mishra, K., Suryanarayana, P., and Iyer, R. M., *in* "Advances in Catalysis Science and Technology" (T. S. R. Prasad Rao, Ed.), p. 1. Wiley Eastern Ltd., New Delhi, 1985.
26. Hirata, T., *J. Less-Common Met.* **107,** 23 (1985).
27. Hirata, T., *J. Less-Common Met.* **124,** 11 (1986).
28. Gupta, N. M., Kamble, V. S., and Iyer, R. M., *Radiat. Phys. Chem.* **12,** 143 (1978).
29. Gupta, N. M., Kamble, V. S., Kulshreshtha, S. K., and Iyer, R. M., to be published.
30. Gupta, N. M., Kamble, V. S., Annaji Rao, K., and Iyer, R. M., *J. Catal.* **60,** 57 (1979).
31. Shenoy, G. K., Niarchos, D., Viccaro, P. J., Dunlap, B. D., Aldred, A. T., and Sandrock, G. D., *J. Less-Common Met.* **73,** 171 (1980).
32. Niemantsverdriet, J. W., Flipse, C. F. J., van der Kraan, A. M., and van Loef, J. J., *Appl. Surf. Sci.* **10,** 302 (1982).
33. Reilly, J. J., and Reidinger, F., *J. Less-Common Met.* **85,** 145 (1982).
34. Matsumoto, T., and Amano, M., *Scr. Met.* **15,** 879 (1981).
35. Goodman, D. W., Kelley, R. D., Madey, T. E., and Yates, J. T., *J. Catal.* **63,** 226 (1980).
36. Pande, C. S., Pick, M. A., and Subatim, R. L., *Scr. Met.* **14,** 899 (1981).
37. Vannice, M. A., *J. Catal.* **74,** 199 (1982).
38. Vannice, M. A., *J. Catal.* **37,** 449 (1975).
39. Bianchi, D., Borkar, S., Teule-Gay, F., and Bennett, C. O., *J. Catal.* **82,** 442 (1983).
40. Tau, L. M., and Bennett, C. O., *J. Catal.* **89,** 327 (1984).
41. Biloen, P., and Sachtler, W. M. H., *Adv. Catal.* **30,** 165 (1981).
42. Wang, S. Y., Moon, S. H., and Vannice, M. A., *J. Catal.* **71,** 167 (1981).